Analytical and Bioanalytical Chemistry (2019) 411:6329–6341
https://doi.org/10.1007/s00216-019-01931-x

RESEARCH PAPER

Comprehensive analysis of tara tannins by reversed-phase and hydrophilic interaction chromatography coupled to ion mobility and high-resolution mass spectrometry

Pieter Venter[1] · Harald Pasch[1] · André de Villiers[1]

Received: 11 March 2019 / Revised: 15 April 2019 / Accepted: 17 May 2019 / Published online: 19 June 2019

Abstract

Reversed-phase liquid chromatography (RP-LC) and hydrophilic interaction chromatography (HILIC) methods hyphenated to diode array detection and ion mobility (IM) high-resolution mass spectrometry (HR-MS) were used for the analysis of gallic acid derivatives and gallotannins in a commercial tara extract. UV spectra combined with low and high-collision energy mass spectral data and known RP-LC elution orders allowed the identification of 45 isomeric gallic acid derivatives and gallotannins. The synergy between IM and UV data was found to provide a simple means to determine the number of depsidic bonds and thus to distinguish between positional isomers. IM also facilitated the assignment of individual isomeric species between HILIC and RP-LC separations. For the hydrolysable tannins present in tara, RP-LC provided superior resolution and specificity compared to HILIC. The results reported in this paper highlight the utility of IM in combination with optimised complementary chromatographic separations and HR-MS for the detailed qualitative analysis of hydrolysable tannins in complex mixtures of these compounds.

Keywords Tara · Gallic acid derivatives · Gallotannins · Hydrophilic interaction chromatography (HILIC) · Reversed-phase liquid chromatography (RP-LC) · Ion mobility (IM) spectrometry high-resolution mass spectrometry (HR-MS)

Introduction

Tara polyphenols comprise of gallic acid derivatives [1] composed of a quinic acid esterified to gallic acid moieties (galloylquinic acids (GQAs)) (Fig. 1), which may also further form aryl ester(s) (depsides) with one or more additional gallic acid residues to form gallotannins [2]. A large number of GQA regioisomers which differ in the position(s) and nature of the respective acyl moieties exist in natural products. These compounds are structurally related to chlorogenic acids (caffeoylquinic acids (CQAs)), where the quinic acid core is esterified to caffeic acid units [1]. An important distinguishing feature of GQAs is the depsidic bond formed between gallic acid units in tara gallotannins [1, 3]. GQAs containing depsidic bonds show a characteristic shoulder at 300 nm in their UV spectra, which increases in intensity with the number of depsidic bonds [4].

Tara tannins are mainly used for the tanning of animal hides used in car interiors due to their properties conferring grain cracking resistance [5]. Other potential uses for tara tannins include their application as resins [6, 7], wood adhesives [8], as protection against steel oxidation [9], as rust removers [10] and as natural antibacterials [11].

Due to the large number of regioisomers comprising tara tannins, their analytical characterisation is challenging. Solvent extraction is commonly performed using water and methanol for low molecular weight (MW), and acetone, ethyl acetate or ethanol for high MW gallic acid derivatives [12–14]. For the purification of gallic acid species, fractionation of solvent extracts by size exclusion chromatography (SEC) on Sephadex LH-20 followed by semi-preparative

Published in the topical collection *Close-Up of Current Developments in Ion Mobility Spectrometry* with guest editor Gérard Hopfgartner.

Electronic supplementary material The online version of this article (https://doi.org/10.1007/s00216-019-01931-x) contains supplementary material, which is available to authorized users.

✉ André de Villiers
ajdevill@sun.ac.za

[1] Department of Chemistry and Polymer Science, Stellenbosch University, Private Bag X1, Matieland 7602, South Africa

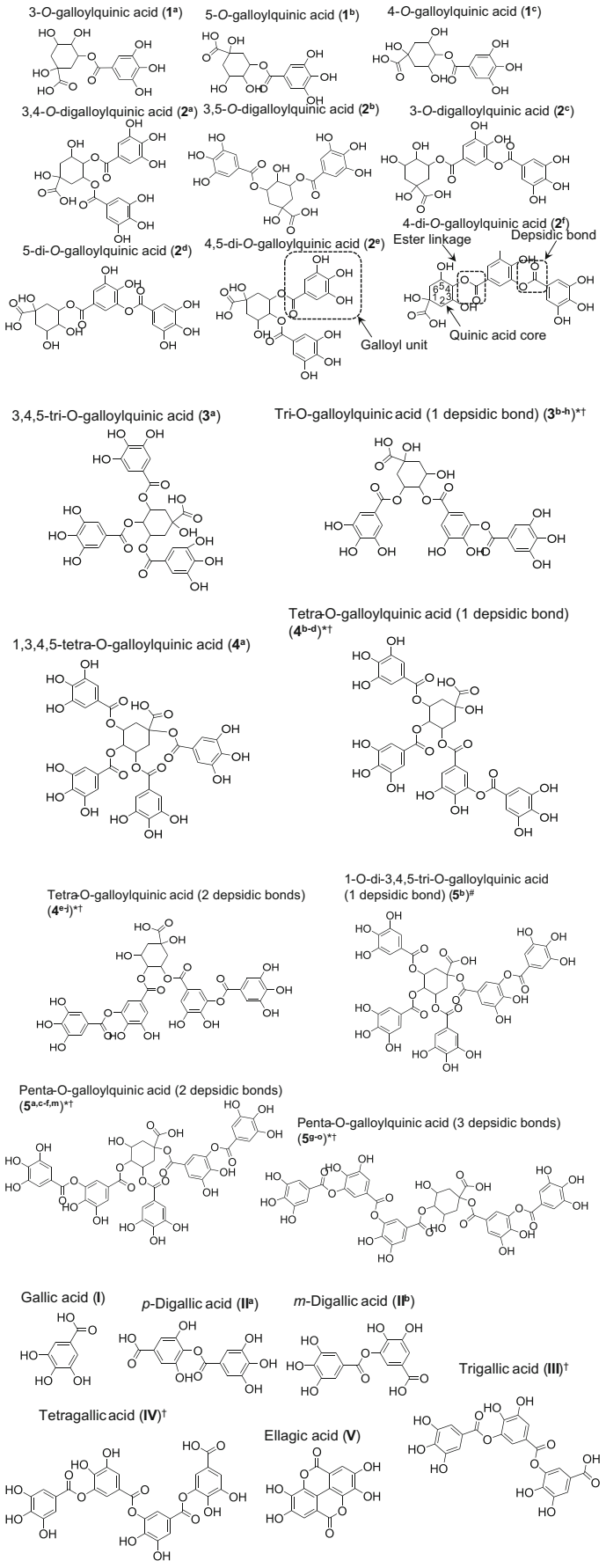
3-O-galloylquinic acid (1a)
5-O-galloylquinic acid (1b)
4-O-galloylquinic acid (1c)
3,4-O-digalloylquinic acid (2a)
3,5-O-digalloylquinic acid (2b)
3-O-digalloylquinic acid (2c)
4-di-O-galloylquinic acid (2f)
Ester linkage
Depsidic bond
5-di-O-galloylquinic acid (2d)
4,5-di-O-galloylquinic acid (2e)
Galloyl unit
Quinic acid core
3,4,5-tri-O-galloylquinic acid (3a)
Tri-O-galloylquinic acid (1 depsidic bond) (3b-h)*†
Tetra-O-galloylquinic acid (1 depsidic bond) (4b-d)*†
1,3,4,5-tetra-O-galloylquinic acid (4a)
Tetra-O-galloylquinic acid (2 depsidic bonds) (4e-j)*†
1-O-di-3,4,5-tri-O-galloylquinic acid (1 depsidic bond) (5b)#
Penta-O-galloylquinic acid (2 depsidic bonds) (5a,c-f,m)*†
Penta-O-galloylquinic acid (3 depsidic bonds) (5g-o)*†
Gallic acid (I)
p-Digallic acid (IIa)
m-Digallic acid (IIb)
Trigallic acid (III)†
Tetragallic acid (IV)†
Ellagic acid (V)

◀ **Fig. 1** Structures of the galloylquinic acid derivatives tentatively identified in the tara extract. Peak labels correspond to Table 1 and Fig. 1; numbers specify the number of galloyl units for each compound and superscript letter distinguish between isomeric species. Compound marked with # are tentatively identified for the first time in tara. For compounds labelled *, representative structures are shown, since regioisomers could not be identified based on the available data. Furthermore, for compounds labelled with a dagger, only representative structures are presented, as *m*- and *p*-isomers could not be distinguished

C18 reversed-phase (RP) isolation is typically used [12, 15, 16]. Normal-phase liquid chromatography (NP-LC) fractionation followed by preparative isolation on a C18 column has also been used for the eventual NMR characterisation of gallic acid derivatives [17]. In terms of analytical separation, NP-LC has been used in the past [18, 19], but reversed-phase liquid chromatography (RP-LC) is nowadays the preferred mode of HPLC for hydrolysable tannins in general [13].

Gallic acid species show a typical UV absorbance band at 280 nm, with a bathochromic shift of 10–12 nm depending on the degree of galloylation. For mass spectrometric identification, negative electrospray ionisation is generally employed [13], with typical fragmentation involving successive neutral losses of galloyl groups (− 152 amu), and both quinic acid (*m*/*z* 191) and gallic acid (*m*/*z* 169) moieties are detected as fragment ions [20]. Clifford and co-workers [21, 22] reported a fragmentation scheme to discriminate between chlorogenic acid regioisomers, which was subsequently also applied to the identification of GQAs in tara [20]. The same relative RP-LC elution order was noted for both mono- and diacylquinic acids, regardless of the chemical nature of the acyl unit [20, 21, 23, 24].

Due to its ability to produce mainly singly charged ions, matrix-assisted laser desorption/ionisation time-of-flight mass spectrometry (MALDI-TOF-MS) has been used to determine the molecular weight distribution of protein-(tara)tannin complexes [25]. This work showed that in tara, quinic acid can be substituted with up to eight galloyl units. Pizzi et al. [26] hypothesised that tara tannins could include structures comprising an ellagic acid core esterified to gallic acid with an additional CO_2 unit, although the limited resolution of the TOF instrument used made distinction between these species and GQAs difficult.

More recently, ion mobility MS (IM-MS) has also found application in the analysis of ellagitannins [27, 28] and chlorogenic acids [29–31]. Ion mobility proved useful for the separation of chlorogenic acid regioisomers as well as prototropic isomers differing their deprotonation sites [30]. Zheng et al. [31] recently reported the use of drift tube ion mobility and a newly developed ultra-high-resolution IM system (structures for lossless ion manipulations (SLIM)) to successfully differentiate between *cis*/*trans*-dicaffeoylquinic acid isomers.

In this study, we report an analytical approach based on hydrophilic interaction chromatography (HILIC) and RP-LC methods hyphenated to diode array detection and travelling wave ion mobility (TWIM) HR-MS for the detailed analysis of tara tannins. We have recently reported the application of a similar approach for the analysis of ellagitannins in chestnut [28]. In the present work, the particular emphasis is on the use of this methodology to distinguish between regioisomeric GQA species found in tara.

Experimental

Materials and reagents

The tara tannin sample, an acetone-water extract of Peruvian tara (*Caesalpinia spinosa*) pods, was obtained from Silvateam (San Michele Mondovì, Italy). HPLC grade acetonitrile, methanol (MeOH) and formic acid were purchased from Sigma-Aldrich (Johannesburg, South Africa), and deionised water was obtained using a Milli-Q water purification system (Millipore, Milford, MA, USA). Poly-DL-alanine used for IM calibration was purchased from Sigma-Aldrich.

Instrumentation and chromatographic conditions

Analyses were performed on an Acquity UPLC system hyphenated to a photodiode array (PDA) detector (500 nL flow cell, 10 mm path length) and a Synapt G2 quadrupole time-of-flight (Q-TOF) mass spectrometer equipped with an ESI source operated in negative ionisation mode (Waters, Milford, MA, USA). UV spectra were recorded from 230 to 500 nm at an acquisition rate of 20 Hz. The MS scan range was 100–2000 amu at a scan time of 0.2 s, with a capillary voltage of − 2.5 kV, a cone voltage of 15 V, a source temperature of 120 °C and an extraction cone voltage of 4.0 V. Nitrogen was used as the desolvation gas at a flow rate of 650 L/h and a temperature of 275 °C. A collision energy ramp of 10–30 V was used to obtain high-energy LC-MS^E data. A sodium formate solution and leucine enkephalin (*m*/*z* = 554.2615) were used for accurate mass calibration and as lock mass calibrants, respectively.

IM measurements were performed using N_2 as the drift gas at 90 mL/min and mobility T wave velocity and wave height of 448 m/s and 37.1 V, respectively. Helium and N_2 flows of 180 mL/min and 90 mL/min were used for the helium and IM cells, respectively.

Travelling wave collisional cross sections ($^{TW}CCS_{N2}$s, Ω) were calculated according to [32] using poly-DL-alanine as a calibrant [33]. Briefly, corrected arrival times (t''_d) were calculated for each ion by correcting for mass-to-charge ratio (*m*/*z*), charge (*z*) and reduced mass (*μ*) and the exponential factor *X* (determined from a plot of t'_d vs. Ω′). These values were plotted against reported Ω values for poly-DL-aniline ions of *m*/*z* 230–1100 [33], and this calibration curve was used to calculate Ω values of the identified hydrolysable tannins.

For both RP-LC and HILIC separations, acidified water (0.1% formic acid) was used as mobile phase A and acetonitrile as mobile phase B. The tannin sample was prepared by dissolving 12 mg/mL in MeOH. Two microliters was injected in full loop mode using acetonitrile and MeOH/H_2O (50/50, *v*/*v*) as weak and strong needle washes, respectively.

HILIC analyses

HILIC separations were performed on an XBridge Amide (150 mm × 4.6 mm i.d., 2.5 μm d_p) column (Waters) by using a linear gradient of 10–12.5% A (0–20 min) at a flow rate of 1 mL/min. The column effluent was split into 1:3 between the PDA and MS detectors.

RP-LC analyses

Separations were performed on a Kinetex (100 mm × 2.1 mm i.d., 1.7 μm d_p) superficially porous column (Phenomenex, Torrance, USA) using the following linear gradient: 2–20% B (0.0–40 min) and 20% B (40–50 min). The flow rate was 0.4 mL/min, with the total flow directed to the MS source.

Data processing

Data acquisition and processing were performed using MassLynx (v. 4.1) and DriftScope (v. 2.1) software (Waters). Reported mass spectra were filtered as a function of arrival time for both low- and high-collision energy data using DriftScope.

Result and discussion

Chromatographic separation

Base peak ion (BPI) chromatograms obtained for the RP-LC and HILIC-IM-MS analyses of the tara tannin extract are presented in Fig. 2a and b, respectively, where the numbers specify the number of galloyl units and the superscript letters distinguish isomeric species. For the gallic acid derivatives and gallotannins present in tara, HILIC provided relatively poor chromatographic performance compared to RP-LC. Furthermore, for the GQA derivatives, the general HILIC retention order (i.e. increasing retention with an increasing degree of galloylation) was similar to that obtained by RP-LC, since a higher number of galloyl moieties increase both the hydrophobicity (due to the aromatic groups) and polarity (due to hydroxyl groups). However, for regioisomers of the same degree of galloylation, the relative elution order often differs between the separation modes (compare the elution orders of compounds with the same number according to superscripts).

Identification of tara hydrolysable tannins

For the tentative identification of compounds **1**$^{a–c}$, **2**$^{a–f}$, **3**^{a}, **4**^{a} and **5**^{b} in tara (Table 1 and Fig. 1), RP-LC elution orders, UV spectral information and high-resolution, high-energy MS data were compared to previous literature reports [20, 21, 23, 24, 34–36]. UV spectra are useful in the differentiation of GQA structural isomers of the same degree of galloylation, but differing in the number of depsidic bonds, based on the relative absorbance at 300 nm due to the depsidic bond [4]. Concerning RP-LC retention, previous studies have shown that the structurally related monoacyl chlorogenic acids (CQAs) elute in the sequence 3-, 5- and 4-*O*-caffeoylquinic acids [34, 35]. The same elution order has been reported for the positional isomers of monoacyl GQAs in RP-LC [20, 21]. Also for diacylated CQAs and GQAs, an identical RP-LC elution order is observed in the sequence 3,4-, 3,5- and 4,5-di-*O*-acylquinic acids, irrespective of the nature of the acyl group [20, 21, 23, 24].

The substitution position of the caffeoyl moiety on the quinic acid core in monoacylated CQAs can also be identified by MS^n [21, 36]. High-collision energy fragmentation spectra show a distinctive dehydrated quinic acid fragment ion at *m*/*z* 173 ([quinic acid-H_2O-H]$^-$) when the acyl unit is located on the 4-position (4-*O*-CQA), whereas 3-*O*-CQA is distinguished from the 5-*O*-CQA positional isomer by a comparatively more intense hydroxycinnamic acid (*m*/*z* 179 [caffeic acid-H]$^{1-}$) ion relative to the *m*/*z* 191 ([quinic acid-H]$^{1-}$) base peak ion. On this basis, Clifford et al. [21] derived a protocol to differentiate diacyl CQAs based on MS^n data. 3,5-di-*O*-CQA is easily identified as this compound does not show a dehydrated quinic acid ion at *m*/*z* 173, whereas 3,4-di-*O*-CQA is differentiated from 3,5-di-*O*-CQA by the relative intensity of the caffeic acid ion in the MS^3 spectrum. The likelihood of intact hydroxycinnamic acid ions being formed during fragmentation decreases in the sequence $1 \approx 5 > 3 > 4$ for substituted CQAs [21, 22], with the facile loss of the C5 acyl unit rationalised [22] as being dependant on the site of the negative charge on the precursor ion. Significantly, this behaviour of acylated quinic acid derivatives is independent of the nature of the acyl moiety [20], such that the same protocol could be used to identify GCA derivatives in the present work.

Based on the criteria outlined above, a total of 45 GQAs comprising mono- to pentagalloylated quinic acid positional and structural isomers were identified in tara (Table 1 and Fig. 1), as discussed in more detail in the following sections.

Three monogalloylquinic acid species were identified based on their elution order and MS^E spectra under RP-LC conditions [20]. The last eluting isomer at 2.80 min (**1**^{c}) was identified as 4-*O*-galloylquinic acid, based on the characteristic fragment ion at *m*/*z* 173 in its MS^E spectrum and its relative hydrophobicity. The two remaining isomers eluting at 1.15 min and 2.28 min were identified as 3-*O*-galloylquinic

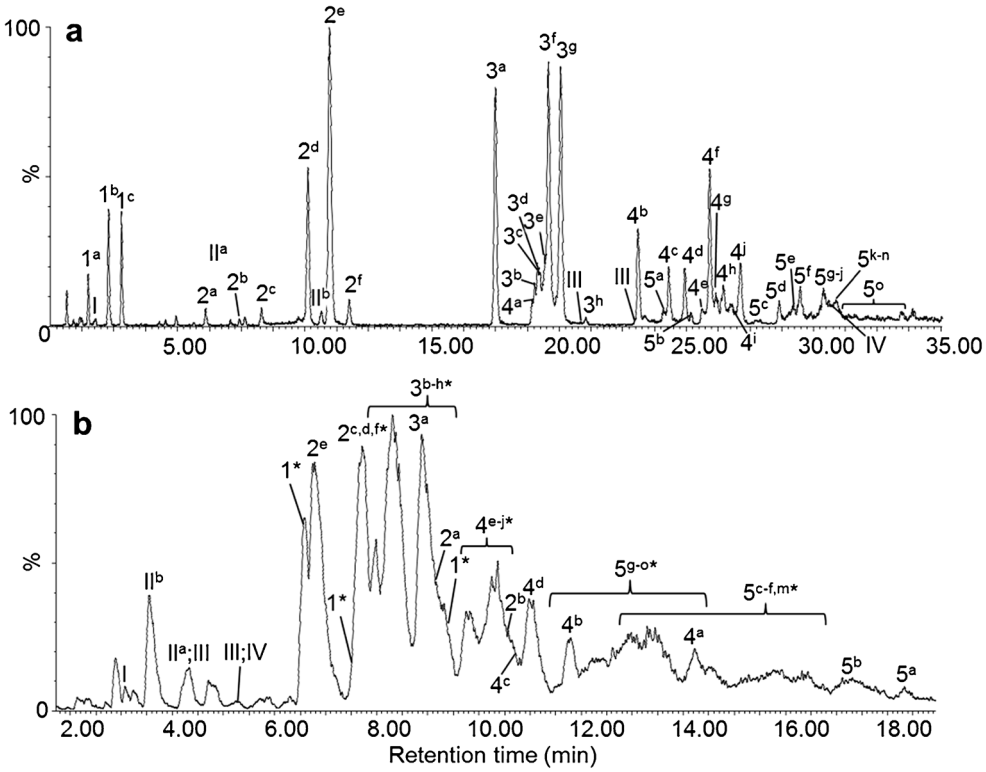

Fig. 2 Base peak ion chromatograms obtained for the (**a**) RP-LC and (**b**) HILIC-IM-Q-TOF-MS analyses of tara hydrolysable tannins. Peak labels correspond to Table 1 and Fig. 1, numbers specify the number of galloyl units for each compound and superscript letters distinguish between isomeric species. * indicates isomers which could not be matched between RP-LC and HILIC. For experimental conditions, refer to the section "Instrumentation and chromatographic conditions"

acid (**1**$^{\mathbf{a}}$) and 5-*O*-galloylquinic acid (**1**$^{\mathbf{b}}$), respectively, taking into account their elution order as well as the low-intensity acyl fragment (*m*/*z* 169) for **1**$^{\mathbf{b}}$. A clean MS^{E} spectrum could not be obtained for 3-*O*-galloylquinic acid under either RP-LC or HILIC conditions due to co-elution, and this compound was therefore solely identified based on RP-LC elution order. To assign the monogalloylquinic acids (**1**$^{\mathbf{a,b,c}}$) in HILIC, the relative peak areas between the two separations were used, which revealed the expected reversed elution order.

Assigning monogalloylquinic acid species between RP-LC and HILIC based on MS^{E} data revealed that the protocol originally developed by Clifford and co-workers [21] for the assignment of CQAs under RP conditions is not suitable as a basis to identify the position of the galloyl unit under HILIC conditions. Comparison of MS^{E} spectra for the two major monogalloylquinic acid isomers obtained under RP-LC (see Electronic Supplementary Material (ESM) Fig. S1) and HILIC (ESM Fig. S2) conditions shows that in the latter case, similar fragment ion intensities are observed, while the fragment ion at *m*/*z* 173, which is diagnostic for all 4-substituted quinic acid derivatives under RP-LC conditions, is also observed for both species. Clifford et al. [22] proposed that the pathways followed by regioisomeric caffeoylquinic acids depend on the position of the negative charge under RP-LC conditions. If this is correct, the apparent loss in mass spectrometric specificity for the monogalloylquinic acid species in HILIC may be a consequence of the negative charge being located on the same position for all three regioisomers, possibly due to a lower polarity [37] or higher effective pH [38, 39] of the organic-rich HILIC mobile phase.

A total of six digalloylquinic acid derivatives were detected and identified based on accurate mass information. Isomers eluting at 8.29 min, 10.12 min and 11.74 min in RP-LC are distinguished by a shoulder at 300 nm in their UV spectra, which points to these compounds containing a depsidic bond and therefore only one site of galloylation. These three regioisomers were characterised by multiple arrival times at 3.10–3.30 ms and 3.60–3.70 ms (refer to Fig. 6 and the following discussion). The last eluting isomer (**2**$^{\mathbf{f}}$, 11.74 min in RP-LC) shows the characteristic dehydrated quinic acid fragment ion at *m*/*z* 173, identifying this compound as 4-di-*O*-digalloylquinic acid (ESM Fig. S3c). The other two isomeric species eluting at 8.29 min and 10.12 min were therefore identified as 3-*O*-galloylquinic acid (**2**$^{\mathbf{c}}$, ESM Fig. S3a) and 5-di-*O*-galloylquinic acid (**2**$^{\mathbf{d}}$, ESM Fig. S3b), respectively, taking into account the elution order of their respective monogalloyl derivatives. Two of the three monodepsidic digalloylquinic acid isomers co-eluted in HILIC, and fragmentation spectra revealed no differences for the peaks at retention times of 7.71 min and 9.01 min (data not shown), so that these isomers could not be distinguished in this separation mode.

For the digalloylquinic acid isomers not containing a depsidic bond, the isomer eluting at 7.12 min in RP-LC was identified as 3,5-di-*O*-galloylquinic acid (**2**$^{\mathbf{b}}$) based on the absence of the dehydrated quinic acid fragment ion (*m*/*z*

Table 1 Galloylquinic acids and gallic acids tentatively identified in tara by RP-LC and HILIC-IM-HR-MS

Compound (no.)	Chemical formula	t_R RP-LC (min)	t_R HILIC (min)	UV (nm)	Exp. mass $[M-H]^{-1}$	Mass error (ppm)	t_d (ms)	$^{TW}CCS_{N2}$ (Å^2)	Fragment ions $[M-H]^{1-}$
3-*O*-Galloylquinic acid (1[a])[#]	$C_{14}H_{16}O_{10}$	1.15	9.48	Co-elution	343.0674	2.62	2.21	170	Co-elution
5-*O*-Galloylquinic acid (1[b])[#]	$C_{14}H_{16}O_{10}$	2.28	7.62	Co-elution	343.0670	1.46	2.21	170	343.0836, 191.0649, 169.0211
4-*O*-Galloylquinic acid (1[c])[#]	$C_{14}H_{16}O_{10}$	2.80	6.59	273	343.0668	0.87	2.21	170	343.0831, 191.0647, 173.0524, 169.0208, 125.0291
3,4-Di-*O*-galloylquinic acid (2[a])	$C_{21}H_{20}O_{14}$	6.10	6.77, 7.71, 9.01, 10.70[#]	Co-elution	495.0784	1.82	3.40	209	495.0770[†], 343.0667, 331.0652, 325.0563, 191.0550, 173.0443, 169.0139
3,5-Di-*O*-galloylquinic acid (2[b])	$C_{21}H_{20}O_{14}$	7.12		Co-elution	495.0777	0.40	3.40	209	343.0679, 331.0694, 191.0540, 169.0130[†], 125.0237
3-*O*-Digalloylquinic acid (2[c])	$C_{21}H_{20}O_{14}$	8.29		281[sh]	495.0775	0.00	3.10 3.60	199 215	495.0770, 365.0497, 343.0667, 191.0550[†], 169.0143, 125.0219
5-*O*-Digalloylquinic acid (2[d])	$C_{21}H_{20}O_{14}$	10.12		272[sh]	495.0794	3.84	3.10 3.60	199 215	495.0782, 365.0498, 343.0672, 325.0568, 191.0550[†], 169.0137
4,5-Di-*O*-galloylquinic acid (2[e])	$C_{21}H_{20}O_{14}$	10.97		276	495.0792	3.43	3.15	201	495.0793[†], 343.0669, 325.0562, 191.0550, 173.0449, 169.0133, 125.0233
4-*O*-Digalloylquinic acid (2[f])	$C_{21}H_{20}O_{14}$	11.74		270[sh]	495.0776	0.20	3.30 3.70	206 218	495.0761, 365.0478, 343.0654[†], 191.0565, 173.0430, 169.0131, 125.0225
3,4,5-Tri-*O*-galloylquinic acid (3[a])	$C_{28}H_{24}O_{18}$	17.48	8.90	275[sh]	647.0887	0.46	4.00	226	647.0939[†], 495.0818, 477.0698, 343.0674, 325.0574, 169.0139
Trigalloylquinic acid (1 depsidic bond) (3[b–h])	$C_{28}H_{24}O_{18}$	19.03, 19.14, 19.22, 19.44, 19.57, 20.05, 21.05	7.98, 8.30, 9.31[#]	276[sh] 273[sh] 275[sh] 273[sh]	647.0903 647.0904 647.0908 647.0890	2.94 3.09 3.71 0.93	4.35 4.35 4.35 4.35	236 236 236 236	647.0891, 495.0787[†], 343.0666, 325.0561, 191.0550, 169.0131
1,3,4,5-Tetra-*O*-galloylquinic acid (4[a])	$C_{35}H_{28}O_{22}$	18.94	14.39	275	799.0992	0.25	4.76	246	799.1014[†], 647.0888, 629.0783, 601.0839, 495.0776, 477.0672, 191.0532, 169.0118
Tetragalloylquinic acid with 1 depsidic bond (4[b])	$C_{35}H_{28}O_{22}$	23.09	11.79	274[sh]	799.1028	4.25	5.04	253	799.0979, 647.0874[†], 495.0767, 169.0125
Tetragalloylquinic acid with 1 depsidic bond (4[c])		24.31	10.57		799.1012	2.25	5.11	255	
Tetragalloylquinic acid with 1 depsidic bond (4[d])		24.93	11.06		799.0999	0.63	5.24	258	
Tetragalloylquinic acid (2 depsidic bonds) (4[e–j])	$C_{35}H_{28}O_{23}$	25.62, 25.91, 26.15, 26.45, 26.78, 27.11	9.46, 9.81, 10.36	272[sh]	799.0996	0.25	5.66	268	799.1007, 647.0910[†], 495.0794, 343.0674, 173.0435, 169.0128
Pentagalloylquinic acid (2 depsidic bonds) (5[a])	$C_{42}H_{32}O_{26}$	24.28	18.31	275[sh]	951.1125	2.21	6.28	282	951.1108, 799.0971, 647.0881[†], 495.0754, 477.0647, 325.0558, 169.0124
1-*O*-Digalloyl-3,4,5-tri-*O*-galloylquinic acid (5[b])	$C_{42}H_{32}O_{26}$	25.19	17.06	275[sh]	951.1116	1.26	5.80	282	951.1115, 799.1005, 647.0894, 629.0779, 601.0848, 495.0775, 477.0696, 325.0533, 169.0138[†]

Table 1 (continued)

Compound (no.)	Chemical formula	t_R RP-LC (min)	t_R HILIC (min)	UV (nm)	Exp. mass $[M-H]^{-1}$	Mass error (ppm)	t_d (ms)	$^{TW}CCS_{N2}$ (Å^2)	Fragment ions $[M-H]^{1-}$
Pentagalloylquinic acid (2 depsidic bonds) ($5^{c-f,m}$)	$C_{42}H_{32}O_{26}$	27.70, 28.65, 29.20, 29.46, 30.80	12.98, 13.42, 14.28, 18.31	274^{sh}	951.1107	0.32	6.28	282	951.1152, 799.1005†, 647.0899, 495.0758, 323.0408, 173.0442, 169.0131
Pentagalloylquinic acid (3 depsidic bonds) (5^{g-o})	$C_{42}H_{32}O_{26}$	30.40, 30.80, 30.90	11.72–12.28	273^{sh}	951.1104	0.00	7.04	299	951.1085, 799.0965†, 647.0848, 495.0755, 323.0396, 173.0442, 169.0117
Gallic acid (I)	$C_7H_6O_5$	1.72	3.06	271	169.0137	2.96	0.83	107	125.0232
p-Digallic acid (II^a)$^{\#}$	$C_{14}H_{10}O_9$	7.10	4.32	270^{sh}	321.0247	1.56	2.00	162	125.0290, 169.0205
m-Digallic acid (II^b)$^{\#}$		10.62	3.53						
Trigallic acid (III)$^{\#}$	$C_{21}H_{14}O_{13}$	20.78	5.15	269^{sh}	473.0360	0.42	3.17	202	321.0377, 169.0211, 125.0306
		22.96	4.30				3.17	202	
		n.d.	4.60				2.90	195	
Tetragallic acid (IV)	$C_{28}H_{18}O_{17}$	31.14	5.27	Co-elution	625.0466	0.80	4.21	232	Co-elution
Ellagic acid (V)	$C_{14}H_6O_8$	23.68	2.90	253, 364	300.9987	− 1.00	1.66	147	283.9947, 257.0065, 245.0087, 229.0147, 217.0122, 201.0180, 173.0251, 145.0271

t_d is the arrival time; co-elution means no clear fragments were obtained due to co-elution

sh shoulder

$^{\#}$ Individual isomeric species were assigned according to their respective peak areas

† Base peak ion in the MS^E spectrum

173) in its MS^E spectrum (ESM Fig. S4b). The two remaining isomers could not be differentiated based on the available MS data. However, taking into account the relative elution order for these isomers reported on a phenyl-hexyl RP column [21], the isomers eluting at 6.10 min and 10.97 min in RP-LC were tentatively identified as 3,4-di-*O*-galloylquinic acid (**2**$^{\mathbf{a}}$, ESM Fig. S4a) and 4,5-di-*O*-galloylquinic acid (**2**$^{\mathbf{e}}$, ESM Fig. S4c), respectively.

Eight trigalloylquinic acid derivatives were identified based on HR-MS data. The first isomer to elute under RP-LC conditions showed no shoulder at 300 nm in its UV spectrum, identifying this component as 3,4,5-tri-*O*-galloylquinic acid (**3**$^{\mathbf{a}}$, ESM Fig. S5f). The later eluting isomers showed an increase in arrival time in IM from 4.00 to 4.35 ms and a shoulder at 300 nm in their UV spectra (ESM Fig. S5g). Comparing the HILIC × IM (ESM Fig. S5a) and RP-LC × IM (ESM Fig. S5b) contour plots allowed for straightforward identification of 3,4,5-tri-*O*-galloylquinic acid in HILIC due to its unique arrival time at 4.00 ms. The MS^E spectra (ESM Fig. S6) of this isomer in both HILIC and RP-LC are unique due to the presence of an extra fragment ion at *m/z* 477 ([M-galloyl-H_2O-H]$^{1-}$), which is also evident in the high-energy spectrum of 1,3,4,5-tetra-*O*-galloylquinic acid (**4**$^{\mathbf{a}}$, see further) [20]. The remaining trigalloyl species (**3**$^{\mathbf{b-h}}$) all produced the same fragmentation spectra in RP-LC (ESM Fig. S7a). Since seven of these isomers were resolved by RP-LC compared to only three in HILIC and identical arrival times were measured for these, assignment of individual species between HILIC and RP-LC was not possible.

The MS^E spectra obtained for the GQAs in tara generally showed more extensive fragmentation under HILIC compared to RP-LC conditions, which may prove beneficial in some cases. For example, different from the case for monogalloylquinic acid species, the diagnostic intensities of ions at *m/z* 169, 173 and 191 for the trigalloylquinic acid isomer eluting at 9.30 min in HILIC allowed for identification of the galloylation positions as 3 and 5 due to the absence of the *m/z* 173 peak, although the position of the depsidic bond could not be determined (ESM Fig. S7c). This observation suggests that when comparable MS data between RP-LC and HILIC are required, such as for library searching for example, higher collision energies should be used in RP-LC.

A total of ten tetragalloylquinic acid derivatives were detected in the tara extract. The isomer eluting first in RP-LC was easy to assign as 1,3,4,5-tetra-*O*-galloylquinic acid (**4**$^{\mathbf{a}}$) by the absence of a shoulder at 300 nm in its UV spectrum and the fact that this compound showed the shortest arrival time of 4.76 ms (refer to Fig. 3). This is further supported by the unique fragmentation behaviour of this isomer, which exhibits an ion at *m/z* 601 ([M-galloyl-CO_2H-H]$^{1-}$, 0.5 ppm) under MS^E conditions [20] (ESM Fig. S8).

IM provided valuable complementary information to RP-LC and HILIC separations regarding the number of depsidic bonds, which, together with HR-MS^E data, greatly facilitated the tentative identification of positional isomers. As an example, the extracted ion HILIC and RP-LC × ion mobility contour plots for tetragalloylquinic acid species (*m/z* 799, [M −H]$^-$) are shown in Fig. 3. 1,3,4,5-Tetra-*O*-galloylquinic acid (**4**$^{\mathbf{a}}$, Fig. 3f), identified as discussed above, showed the shortest arrival time of all tetra-*O*-galloylquinic acid derivatives at 4.76 ms. Two additional arrival time clusters where recorded at 5.04–5.24 ms and 5.66 ms, respectively (Fig. 3c), both coinciding with an increasingly evident shoulder at 300 nm in the UV spectra of the respective peaks (Fig. 3g, h). (A similar increase in arrival time and relative absorbance at 300 nm as a function of number of depsidic bonds was observed for tri- and penta-*O*-galloylquinic acid species; Fig. S5 (see ESM) and Fig. 5, respectively). This indicates, as expected, that the effective $^{TW}CCS_{N2}$ values of GQA derivatives increase with the number of depsidic bonds (Table 1). The complementary information provided by UV and IM data therefore provides a simple means of distinguishing between positional isomers containing different numbers of depsidic bonds. Furthermore, the characteristic arrival times for particular positional isomers facilitated assignment of individual isomeric species of di-, tri-, tetra- and pentagalloylquinic acids between HILIC and RP-LC (Figs. 6, S5 (see ESM), 3 and 5, respectively), which generally showed an inverse elution order. For example, minor differences in arrival time were measured for regioisomeric tetragalloylquinic acid species (Fig. 3) which contain one depsidic bond (**4**$^{\mathbf{b}}$, **4**$^{\mathbf{c}}$ and **4**$^{\mathbf{d}}$), indicating that **4**$^{\mathbf{c}}$ and **4**$^{\mathbf{d}}$ retain the same elution order in HILIC and RP-LC. Although no further information regarding the substitution patterns could be obtained, IM offered partial differentiation between these isomeric species, which was not possible based on MS data alone (ESM Fig. S9).

Based on the criteria outlined above, tetragalloylquinic acid derivatives **4**$^{\mathbf{b-d}}$ could be assigned as containing a single depsidic bond, while compounds **4**$^{\mathbf{e-j}}$ contained two depsidic bonds. Unlike **4**$^{\mathbf{b-d}}$, however, the isomers containing two depsidic bonds showed nearly identical arrival times (5.66 ms) and fragmentation behaviour, and, especially in HILIC, extensive co-elution. As a consequence, assignment of individual isomers was not possible for these isomers.

Fifteen pentagalloylquinic acid derivatives were identified by HR-MS (*m/z* 951, $C_{42}H_{31}O_{26}$). The pentagalloylquinic acid isomers eluting at 24.28 min (**5**$^{\mathbf{a}}$) and 25.19 min (**5**$^{\mathbf{b}}$) in RP-LC and 17.06 min (**5**$^{\mathbf{b}}$) and 18.31 min (**5**$^{\mathbf{a}}$) in HILIC produce a characteristic ion at *m/z* 601 ([M-2galloyl-CO_2H-H]$^{1-}$, 0.5 ppm) under MS^E conditions (Fig. 4), indicating that an *O*-digalloyl group containing one depsidic bond is attached to quinic acid at position 1 for both isomers [20]. The formation of fragment ions *m/z* 647 ([M-2galloyl-H]$^{1-}$), *m/z* 601 ([M-2galloyl-CO_2H-H]$^{1-}$) and *m/z* 629 ([M-2galloyl-H_2O-H]$^{1-}$) can be explained by an acyl transfer mechanism (ESM Fig. S10, adapted from Scheme B in [22]). However, no

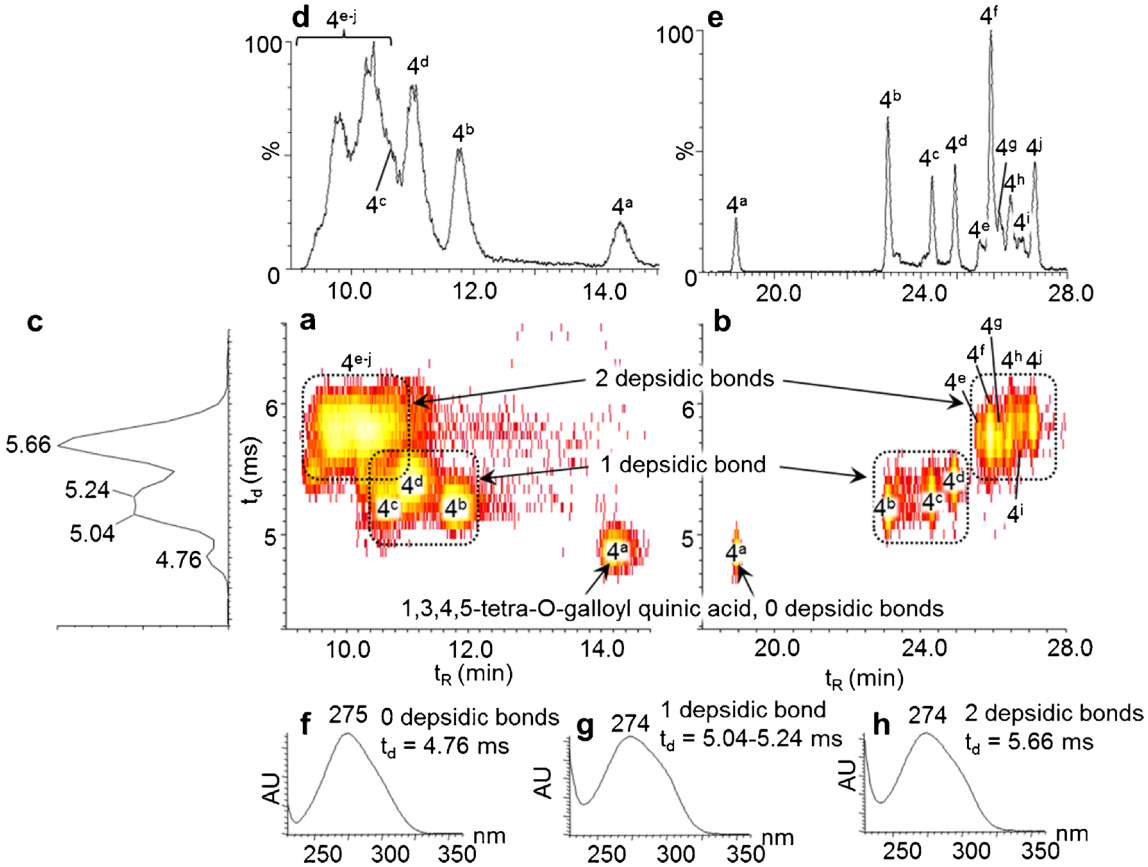

Fig. 3 Extracted ion HILIC × ion mobility (**a**) and RP-LC × ion mobility (**b**) contour plots for tetragalloylquinic acid derivatives (*m/z* 799) in tara. Panel (**c**) shows the corresponding extracted ion arrival time plot (identical for HILIC and RP-LC), panels (**d**) and (**e**) the corresponding extracted ion chromatograms for HILIC and RP-LC and inserts (**f**)–(**h**) the representative UV spectra of each of the positional isomers containing 1, 2 or 3 depsidic bonds, respectively. Compound numbers correspond to Table 1

further information regarding the nature of the remainder of acyl groups could be obtained by either MS or UV data. The key to distinguishing between these isomers is the longer arrival time of **5**^{a} (6.28 ms vs. 5.80 ms for **5**^{b}), which indicates

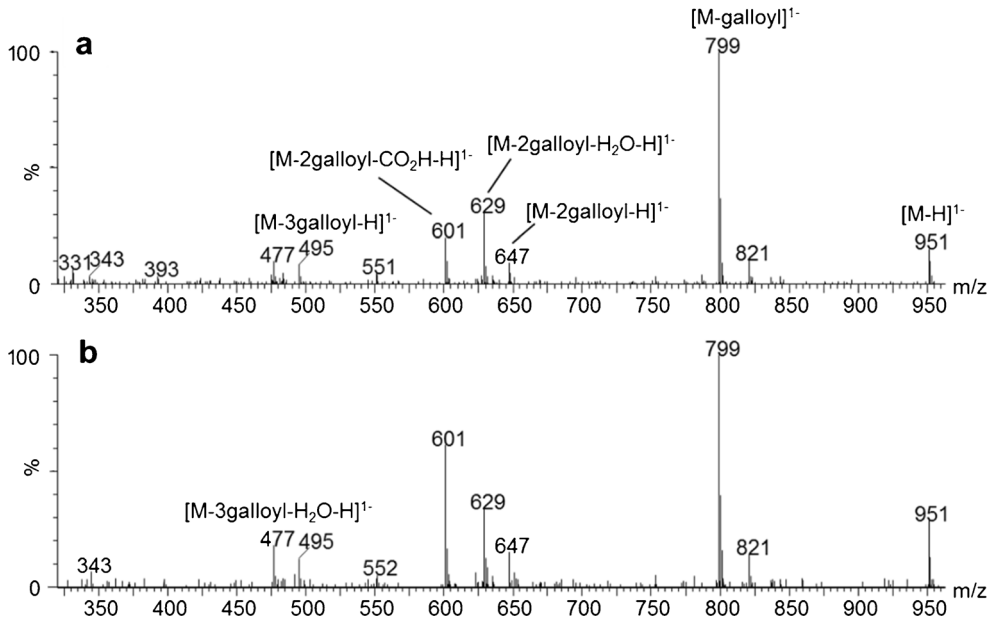

Fig. 4 MS^{E} spectra obtained for pentagalloylquinic acid isomers eluting at 17.06 min (**a**, **5**^{b}) and 18.31 min (**b**, **5**^{a}) under HILIC conditions

that this compound contains an additional depsidic bond, although its position could not be ascertained (Fig. 5). Based on this information, **5**$^{\mathbf{b}}$ was tentatively identified as 1-di-*O*-galloyl-3,4,5-tri-*O*-galloylquinic acid, while **5**$^{\mathbf{a}}$ contains a second depsidic chain at position 3, 4 or 5 on the quinic acid core.

The fragmentation spectra for the remaining pentagalloylquinic acid species at arrival times of 6.28 ms and 7.04 ms, representing isomers containing 2 and 3 depsidic bonds, respectively, were very similar (ESM Fig. S11). The only noticeable difference is the higher abundance of the fragment ion at *m/z* 495 $[M\text{-}3galloyl\text{-}H]^-$ in the MS^E spectra of the species containing 3 depsidic bonds ($t_d = 7.04$ ms), indicating that a cleavage of depsidic chains occurs more readily than single *O*-galloyl groups.

Multiple arrival times (3.10~3.30 ms and 3.60~3.70 ms) were observed for each of the digalloylquinic acid isomers containing a single depsidic bond (**2**$^{\mathbf{c}}$, **2**$^{\mathbf{d}}$ and **2**$^{\mathbf{f}}$), as shown in Fig. 6. Since the positions of the depsidic bonds for each of these compounds have been ascertained based on MS data, the two species resolved for each compound by IM do not correspond to positional isomers. Rather, the species resolved by IM likely correspond to either prototropic isomers differing in the position of their negative charges [30, 37] or to structural isomers containing *m*- and *p*-depsidic bonds, respectively [18]. MS^E spectra for each of the IM-resolved species filtered according to arrival time are presented in Fig. S12 (see ESM). These indicate no discernible differences between the species separated by IM, with the exception of the higher prevalence of sodium and potassium adducts for the 4-*O*-digalloylquinic acid species and especially the 5-*O*-digalloylquinic acid species with the later arrival times (Fig. S12, b1 and c1).

Considering that the *m*- and *p*-isomers of digallic acid are quite well separated in both HILIC and RP-LC (Fig. 2, **II**$^{\mathbf{a,b}}$) and that IM did not provide differentiation of these species (see in the following), the fact that no chromatographic separation of the IM-resolved digalloylquinic acid species is evident in either separation mode implies that these more likely correspond to prototropic isomers, although this could not be conclusively proven based on the available data.

In general, the results reported in the present work for galloylquinic acids compare well with a previous study of structurally related chlorogenic acid regioisomers [31] in terms of relative IM behaviour. 4,5-Di-*O*-caffeoylquinic acid and the structurally related 4,5-di-*O*-galloylquinic acid (**2**$^{\mathbf{e}}$) in

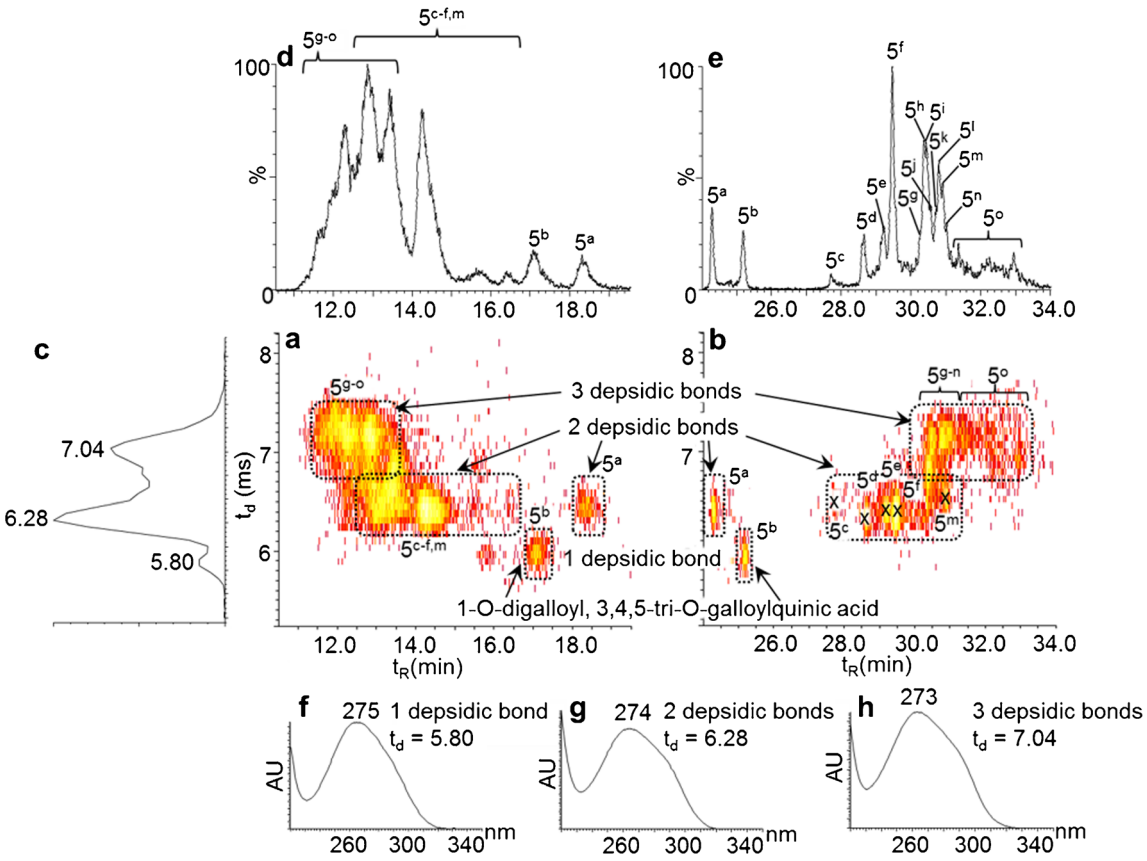

Fig. 5 Extracted ion HILIC × ion mobility (**a**) and RP-LC × ion mobility (**b**) contour plots for pentagalloylquinic acid derivatives in tara. Panel (**c**) shows the corresponding extracted ion arrival time plot (identical for HILIC and RP-LC), panels (**d**) and (**e**) the corresponding extracted ion chromatograms for HILIC and RP-LC and inserts (**f**)–(**h**) the representative UV spectra of positional isomers containing 1, 2 or 3 depsidic bonds, respectively. Compound numbers correspond to Table 1

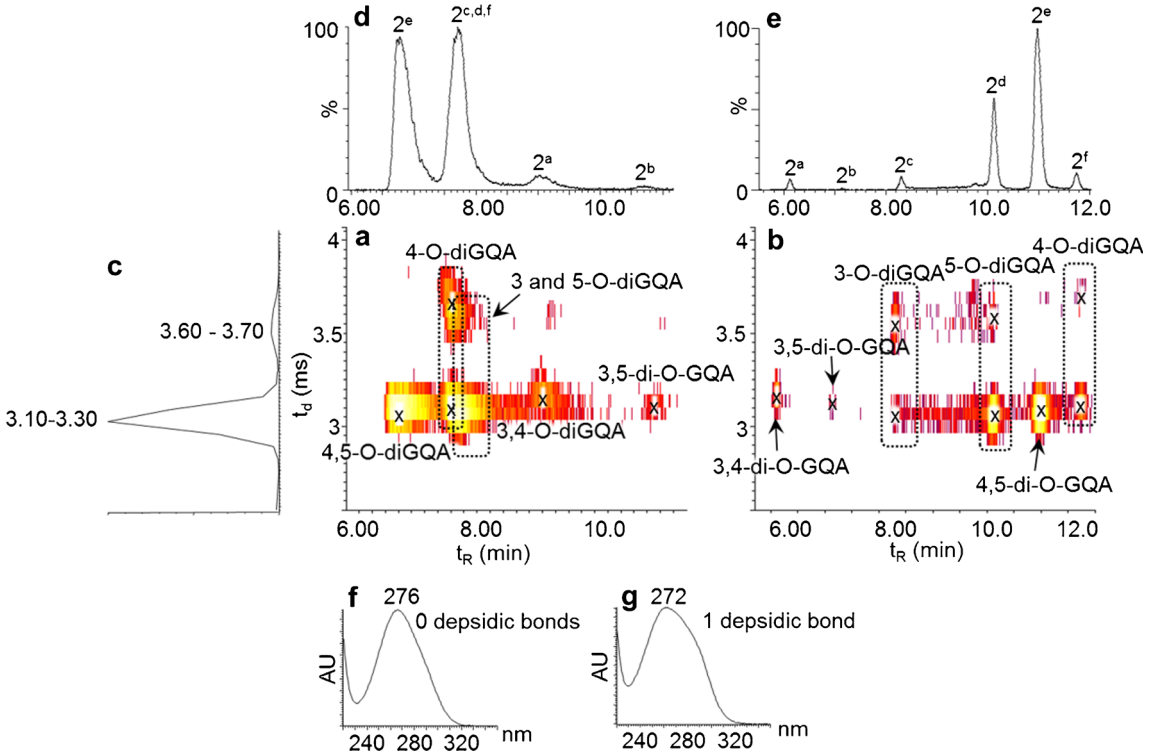

Fig. 6 Extracted ion HILIC × ion mobility (**a**) and RP-LC × ion mobility (**b**) contour plots for digalloylquinic acid (diGQA) derivatives in tara. Panel (**c**) shows the corresponding extracted ion arrival time plot (identical for HILIC and RP-LC), panels (**d**) and (**e**) the corresponding extracted ion chromatograms for HILIC and RP-LC and inserts (**f**) and (**g**) the representative UV spectra of positional isomers containing one and no depsidic bonds, respectively. Compound numbers correspond to Table 1

tara both showed shorter arrival times relative to the respective 3,4- and 3,5-di-*O*-acylquinic acid species, which made it possible to assign individual non-depsidic digalloylquinic acid species between HILIC and RP-LC (Fig. 6). It was straightforward to assign the depsidic digalloylquinic acid isomers in HILIC compared to RP-LC due to the multiple arrival times observed for the proposed prototropic isomers, which subsequently indicated all three depsidic isomers (**2**^{c}, **2**^{d} and **2**^{f}) co-eluted in HILIC (Fig. 6).

For several of the di-, tetra- and penta-*O*-galloylquinic acid derivatives (**2**^{c,d}, **4**^{b,c,d}, **5**^{a,b}), evidence of on-column conversion between species was observed in RP-LC, as reflected by a characteristic-raised baseline (peak–plateau–peak) between species in the relevant extracted ion chromatograms (ESM Fig. S13). This phenomenon is well known for chiral compounds [40, 41] and has been observed previously, although not addressed in detail, for tara polyphenols [20]. Although not clearly evident in HILIC, this might be due to the relatively poor chromatographic performance of the technique. These interconversion reactions likely correspond to on-column conversions between the relevant positional isomers (e.g. between 3- and 5-di-*O*-galloylquinic acid (**2**^{c} and **2**^{d}) and between tetragalloylquinic acid species with one depsidic bond (**4**^{b,c,d})). The pentagalloylquinic acid derivatives **5**^{a} and **5**^{b} with unique arrival times at 6.28 ms and 5.80 ms also show this characteristic raised baseline due to on-column conversion (ESM Fig. S13c). If **5**^{b} (t_d = 5.80 ms) is indeed 1-di-*O*-digalloyl-3,4,5-tri-*O*-galloylquinic acid, which converts to **5**^{a} (t_d = 6.28 ms) containing two depsidic bonds, this provides evidence that galloyl units are capable of migrating not only to different positions on the quinic acid core but also to phenolic groups on (presumably adjacent) galloyl units. In IM, the interconverting species representing the raised baseline not surprisingly showed the same arrival time as the corresponding isomers (Fig. 6).

Finally, several gallic acid derivatives were also detected in tara, including gallic acid (**I**), digallic acid (**II**), trigallic acid (**III**) and tetragallic acid (**IV**) (Fig. 1). The presence of these compounds is likely a consequence of the hydrolysis of GQAs. The di- and trigallic acid species showed the expected shoulder at 300 nm in their UV spectra due to the depsidic bond(s) (it was not possible to obtain a clean UV spectrum for tetragallic acid due to co-elution). These compounds were characterised by simple fragmentation patterns, with MS^{E} spectra showing losses of galloyl groups and both deprotonated (*m*/*z* 169) and decarboxylated (*m*/*z* 125) gallic acid ions.

Two chromatographic peaks were observed for both digallic acid (**II**) and trigallic acid (**III**) in both HILIC and RP-LC. Identical arrival times were measured for these species (Table 1). For digallic acid, the two peaks correspond to *m*- and *p*-depsidic isomers, with *p*-digallic acid eluting before

m-digallic acid in RP-LC [42]. It has been shown that *m*-digallic acid is converted to *p*-digallic acid in methanol [18]. Since the tara sample was dissolved in methanol, such a conversion may be responsible for the detection of *p*-digallic acid in this work. Furthermore, oxidation of *m*-digallic acid has been shown to results in the formation of ellagic acid (**V**) [43], which was identified based on HR-MS^E and UV spectral data [4, 28, 44]. For trigallic acid, three of the four possible isomers (*m-p*, *p-m*, *m-m* and *p-p*) were observed in HILIC and only two in RP-LC. These two peaks could be assigned between the separation modes based on their relative peak areas, since both showed identical arrival times. The third trigallic acid species, detected only in HILIC, showed a slightly shorter arrival time. Only a single peak of very low intensity was observed to tetragallic acid (**IV**) in both HILIC and RP-LC.

Conclusions

Comprehensive analysis of a commercial tara extract by RP-LC and HILIC coupled to diode array detection and IM-HR-MS allowed for the tentative identification of 45 isomeric galloylquinic acid species in addition to six gallic acid derivatives and ellagic acid. RP-LC provided superior separation for tara tannins compared to HILIC. The complimentary information provided by the combination of UV spectral data and IM separation provided a facile methodology to identify the number of depsidic bonds and thereby to differentiate between positional isomers of the same degree of galloylation. Characteristic arrival time differences allowed in most cases for the assignment of individual isomeric species between HILIC and RP-LC. The proposed presence of prototropic isomers explains the loss in mass spectrometric specificity for the monogalloylquinic acid species as well as multiple IM arrival times for the di-*O*-galloylquinic acid isomers. Evidence of on-column conversion between species was observed in RP-LC, where the combination of IM and chromatographic data suggests the migration of galloyl groups to different positions on the quinic acid core as well as to galloyl phenolic groups. The results of the present study for tara tannins confirm the utility of an analytical methodology based on the combination of RP-LC and HILIC separation with IM and HR-MS for the comprehensive analysis of hydrolysable tannins. Future work should include the use of commercial reference standards, where available, to confirm the tentative assignments reported in the present work.

Acknowledgements The authors gratefully acknowledge Prof. A. Pizzi for providing the tannin sample.

Funding information This study was financially supported by Sasol (SASOL Chair grant to HP, collaborative grant to AdV) and the National Research Foundation (NRF, grant 98897 to AdV, bursary to PV).

Compliance with ethical standards

Conflict of interest The authors declare that they have no conflict of interest.

References

1. Haslam E, Haworth RD, Keen PC. Gallotannins. Part VII. Tara gallotannin. J Chem Soc. 1962:3814–8.
2. Gross GG. From lignins to tannins: forty years of enzyme studies on the biosynthesis of phenolic compounds. Phytochemistry. 2008;69:3018–31. https://doi.org/10.1016/j.phytochem.2007.04.031.
3. Armitage R, Bayliss GS, Gramshaw JW, Haslam E, Haworth RD, Jones K, et al. Gallotannins. Part III.* The constitution of Chinese, Turkish, Sumach, and tara tannins. J Chem Soc Perkin Trans. 1961;2:1842–53.
4. Arapitsas P, Menichetti S, Vincieri FF, Romani A. Hydrolyzable tannins with the hexahydroxydiphenoyl unit and the m-depsidic link: HPLC-DAD-MS identification and model synthesis. J Agric Food Chem. 2007;55:48–55.
5. Martins D, Duarte L, Silva VFM, Crispim A, Beghini E, Crispim F. Study of vegetable extracts effect on wet-white leather. Leather Footwear J. 2018;18:213–8.
6. Lagel MC, Pizzi A, Giovando S. Matrix-assisted laser desorption-ionization time of flight (MALDI-TOF) mass spectrometry of phenol-formaldehyde-chestnut tannin resins. J Renew Mater. 2014;2:207–19.
7. Aouf C, Benyahya S, Esnouf A, Caillol S, Boutevin B, Fulcrand H. Tara tannins as phenolic precursors of thermosetting epoxy resins. Eur Polym J. 2014;55:186–98.
8. Galvez JMG, Riedl B, Conner AH. Analytical studies on tara tannins. Holzforschung. 1997;51:235–43.
9. Zhao B, Han W, Zhang W, Shi B. Corrosion inhibition performance of tannins for mild steel in hydrochloric acid solution. Res Chem Intermed. 2018;44:407–23.
10. Merino SF, Caprari JJ, Torres LV, Ramos LF, Girola AH. Inhibitive action of tara tannin in rust converter formultaion. Anti-Corrosion Methods Mater. 2017;64:136–47.
11. Aguilar-Galvez A, Noratto G, Chambi F, Debaste F, Campos D. Potential of tara (Caesalpinia spinosa) gallotannins and hydrolysates as natural antibacterial compounds. Food Chem. 2014;156:301–4.
12. Tian F, Li B, Ji B, Zhang G, Luo Y. Identification and structure-activity relationship of gallotannins separated from Galla chinensis. LWT Food Sci Technol. 2009;42:1289–95. https://doi.org/10.1016/j.lwt.2009.03.004.
13. Arapitsas P. Hydrolyzable tannin analysis in food. Food Chem. 2012;135:1708–17. https://doi.org/10.1016/j.foodchem.2012.05.096.
14. Mueller-Harvey A. Analysis of hydrolysable tannins. Anim Feed Sci Technol. 2001;91:3–20.
15. Engels C, Knödler M, Zhao YY, Carle R, Gänzle MG, Schieber A. Antimicrobial activity of gallotannins isolated from mango (Mangifera indica L.) kernels. J Agric Food Chem. 2009;57:7712–8. https://doi.org/10.1021/jf901621m.
16. Salminen JP, Ossipov V, Loponen J, Haukioja E, Pihlaja K. Characterisation of hydrolysable tannins from leaves of Betula pubescens by high-performance liquid chromatography-mass spectrometry. J Chromatogr A. 1999;864:283–91. https://doi.org/10.1016/S0021-9673(99)01036-5.
17. Owen RW, Haubner R, Hull WE, Erben G, Spiegelhalder B, Bartsch H, et al. Isolation and structure elucidation of the major individual

polyphenols in carob fibre. Food Chem Toxicol. 2003;41:1727–38. https://doi.org/10.1016/S0278-6915(03)00200-X.
18. Delahaye P, Verzele M. Analysis of gallic, digallic and trigallic acids in tannic acids by high-performance liquid chromatography. J Chromatogr. 1983;265:363–7.
19. Beasley TH, Ziegler HW, Bell AD. Determination and characterization of gallotannin by high performance liquid chromatography. Anal Chem. 1991;49:238–43. https://doi.org/10.1002/bmc.1130050503.
20. Clifford MN, Stoupi S, Kuhnert N. Profiling and characterization by LC-MS of the galloylquinic acids of green tea, tara tannin, and tannic acid. J Agric Food Chem. 2007;55:2797–807.
21. Clifford MN, Johnston KL, Knight S, Kuhnert N. Hierarchical scheme for LC-MSn identification of chlorogenic acids. J Agric Food Chem. 2003;51:2900–11.
22. Clifford MN, Knight S, Kuhnert N. Discriminating between the six isomers of dicaffeoylquinic acid by LC-MSn. J Agric Food Chem. 2005;53:3821–32.
23. Clifford MN. Coffee bean dicaffeoylquinic acids. Phytochemistry. 1986;25:1767–9.
24. Clifford MN, Knight S, Birgul S, Kuhnert N. Characterization by LC-MSn of four new classes of chlorogenic acids in green coffee beans: dimethoxycinnamoylquinic acids, diferuloylquinic acids, caffeoyl-dimethoxycinnamoylquinic acids, and feruloyl-dimethoxycinnamoylquinic acids. J Agric Food Chem. 2006;54:1957–69.
25. Mane C, Sommerer N, Yalcin T, Cheynier V, Cole RB, Fulcrand H. Assessment of the molecular weight distribution of tannin fractions through MALDI-TOF MS analysis of protein−tannin complexes assessment of the molecular weight distribution of tannin fractions through MALDI-TOF MS analysis of protein-tannin complexes. Anal Chem. 2007;79:2239–48.
26. Pizzi A, Pasch H, Rode K, Giovando S. Polymer structure of commercial hydrolyzable tannins by matrix-assisted laser desorption/ionization-time-of-flight mass spectrometry. J Appl Polym Sci. 2009;113:3847–59.
27. Franceschi P, Vrhovsek U, Guella G. Ion mobility mass spectrometric investigation of ellagitannins and their non-covalent aggregates. Rapid Commun Mass Spectrom. 2011;25:827–33.
28. Venter P, Pasch H, de Villiers A. Comprehensive analysis of hydrolysable tannins by reversed phase and hydrophilic interaction chromatography coupled to ion mobility and high-resolution mass spectrometry. Anal Chim Acta. 2019; (submitted).
29. Xie C, Yu K, Zhong D, Yuan T, Ye F, Jarrell JA, et al. Investigation of isomeric transformations of chlorogenic acid in buffers and biological matrixes by ultraperformance liquid chromatography coupled with hybrid quadrupole/ion mobility/orthogonal acceleration time-of-flight mass spectrometry. J Agric Food Chem. 2011;59:11078–87.
30. Kuhnert N, Yassin GH, Jaiswal R, Matei MF, Grün CH. Differentiation of prototropic ions in regioisomeric caffeoyl quinic acids by electrospray ion mobility mass spectrometry. Rapid Commun Mass Spectrom. 2015;29:675–80.
31. Zheng X, Renslow RS, Makola MM, Webb IK, Deng L, Thomas DG, et al. Structural elucidation of cis/trans dicaffeoylquinic acid photoisomerization using ion mobility spectrometry-mass spectrometry. J Phys Chem Lett. 2017;8:1381–8.
32. Ruotolo BT, Benesch JL, Sandercock AM, Hyung S, Robinson CV. Ion mobility-mass spectrometry analysis of large protein complexes. Nat Protoc. 2008;3:1139–52.
33. Forsythe JG, Petrov AS, Walker CA, Allen SJ, Pellissier JS, Bush MF, et al. Collision cross section calibrants for negative ion mode traveling wave ion mobility-mass spectrometry. Analyst. 2015;140:6853–61.
34. Donovan JL, Meyer AS, Waterhouse A. Phenolic composition and antioxidant activity of prunes and prune juice (Prunus domestica) prune juice (Prunus domestica). J Agric Food Chem. 1998;46:1247–52.
35. Nakatani N, Kayano S, Kikuzaki H, Sumino K, Katagiri K. Identification, quantitative determination, and antioxidative activities of chlorogenic acid isomers in prune (Prunus domestica L). J Agric Food Chem. 2000;48:5512–6.
36. Fang N, Yu S, Prior RL. LC/MS/MS characterization of phenolic constituents in dried plums. J Agric Food Chem. 2002;50:3579–85.
37. Warnke S, Seo J, Boschmans J, Sobott F, Scrivens JH, Bleiholder C, et al. Protomers of benzocaine: solvent and permittivity dependence. J Am Chem Soc. 2015;137:4236–42. https://doi.org/10.1021/jacs.5b01338.
38. Gagliardi LG, Castells CB, Ràfols C, Rosés M, Bosch E. δ conversion parameter between pH scales (WSpH and SSPH) in acetonitrile/water mixtures at various compositions and temperatures. Anal Chem. 2007;79:3180–7. https://doi.org/10.1021/ac062372h.
39. Willemse CM, Stander MA, de Villiers A. Hydrophilic interaction chromatographic analysis of anthocyanins. J Chromatogr A. 2013;1319:127–40.
40. Bu X, Skrdla PJ, Dormer PG, Bereznitski Y. Separation of triphenyl atropisomers of a pharmaceutical compound on a novel mixed mode stationary phase: a case study involving dynamic chromatography, dynamic NMR and molecular modeling. J Chromatogr A. 2010;1217:7255–64.
41. Fedurcová A, Vančová M, Mydlová J, Lehotay J, Krupčík J, Armstrong DW. Interconversion of oxazepam enantiomers during HPLC separation. Determination of thermodynamic parameters. J Liq Chromatogr Relat Technol. 2006;29:2889–900.
42. Verzele M, Delahaye P, van Dijck J. Digallic acid. Bull Soc Chim Belg. 1983;92:181–6. https://doi.org/10.1002/bscb.19830920212.
43. Nierenstein M, Spiers CW, Hatcher PR. Gallotannin. XIII. The identity of digallic acid from gallotannins with synthetic meta-digallic acid. J Am Chem Soc. 1925;47:846–50.
44. Jurd L. Plant polyphenols. I. The polyphenolic constituents of the pellicle of the walnut. J Am Chem Soc. 1956;78:3345–448. https://doi.org/10.1021/ja01595a050.